Reconstruction of chaotic sets from transient chaotic time series: An overview for experimentalists

Imre M. Jánosi
Department of Atomic Physics
Eötvös University, Budapest, Puskin u. 5-7, H-1088, Hungary

Tamás Tél
Institute for Theoretical Physics
Eötvös University, Budapest, Puskin u. 5-7, H-1088, Hungary

ABSTRATCT

A simple method is described how nonattracting chaotic sets can be reconstructed from time series by gluing pieces of many transiently chaotic signals together which come close to this invariant set. The method is illustrated with and its validity is checked by a map of well known dynamics, the Hénon map. The nonattracting strange set is reconstructed in the presence of both a periodic and a chaotic attractor. Since the experimental investigation of transient chaos has received little attention, although the phenomenon is quite well understood theoretically, we hope that these findings might motivate further experimental studies.

I. INTRODUCTION

Chaotic transients often occur in nonlinear systems. A trajectory is transiently chaotic if it initially moves around in an apparently chaotic manner and then, rather suddenly, settles down to an attracting motion which is either periodic or chaotic but in this latter case of other type than initially. If one is studying the asymptotic behavior of such systems only, one misses the interesting, chaotic part contained in the transients.

In systems exhibiting transient chaos there exists in phase space a *nonattracting set* called a chaotic saddle or repellor[1,2,3,4], together with an attractor which is either simple, i.e., periodic, or chaotic. Trajectories starting from randomly choosen initial points then approach the attractor with probability one. Before reaching it, however, they might come close to the nonattracting set and stay in its vicinity for a shorter or longer time.

The nonattracting chaotic set is called a *chaotic repellor* if it does not possess any basin of attraction, and a *chaotic saddle* if its basin of attraction is a fractal set of measure zero. Both types of strange sets appear to be the closures of an infinity of periodic orbits[5,6,7]. In case of a chaotic repellor (saddle) these orbits are strictly repelling (hyperbolic, i.e., attracting along an invariant manifold but repelling otherwise).

In one-dimensional maps the nonattracting chaotic set can be a repellor only. For our purposes invertible maps are of principal importance since they are associated with time-continuous invertible flows describing physical processes. In such cases the nonattracting set is always a chaotic saddle which will be the main subject of our investigations. A common feature of nonattracting chaotic sets is their pronounced fractal structure. A chaotic repellor in 1D is a kind of Cantor set. A chaotic saddle has a fractal structure along *both* its stable and unstable direction in contrast to a chaotic attractor which is always smooth along its unstable direction.

A typical occurence of transient chaos is in the periodic windows inside the chaotic region. The positivity of the topological entropy then ensures the existence of a nonattracting chaotic set. Such windows occur between two crisis configurations: a boundary crisis[1] (where a chaotic attractor ceases to exists) and an interior crisis[1] (where a chaotic attractor is suddenly enlarged). The attractor beyond boundary crises is a periodic one, say of period–m, but by increasing a system parameter further it typically undergoes a period doubling bifurcation, becomes a chaotic attractor which evolves (via an inverse cascade) into an m–piece chaotic attractor. Consequently, below and above the accumulation point in the window the nonattracting chaotic set coexists with a periodic and a chaotic attractor, respectively.

Trajectories starting from points of a nonattracting set never leave it and exhibit chaotic motion forever. To hit such a point by a random choice is, however, completely unlikely since the set is, together with its basin of attraction, of zero measure, a fractal. What is observable experimentally is not the strange set but rather a *small neighborhood* of it and of its stable manifold. Trajectories starting close to the strange set or its attracting manifold can stay for a long time in a neighborhood of the set and show chaotic properties, but sooner or later they escape. These are the trajectories producing transiently chaotic signals.

II. TIME SERIES ANALYSIS OF TRANSIENT CHAOS

Our aim is to study how nonattracting chaotic sets can be reconstructed from time series. Suppose, we follow one single variable (x) of the system and record the data as a time series.

In this paper we use the well-known Hénon map

$$x_{n+1} = 1 - ax_n^2 + by_n \qquad y_{n+1} = x_n \tag{1}$$

with different parameter sets for illustration. This is the most general form of invertible quadratic maps and reflects, thus, faithfully the dynamics associated with systems described by ordinary differential equations. The map is only used here as a generator of transient chaotic time series which are then analyzed exactly in the same manner as in experimental situations.

The main steps of the algorithm are as follows:

1. Take an ensemble of time series containing transients to a steady state behavior.

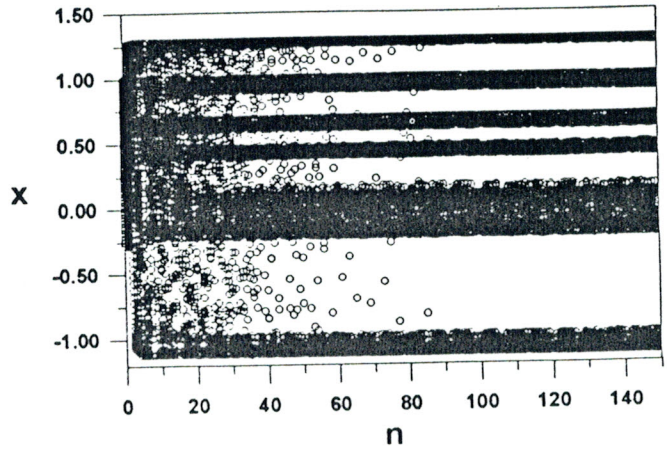

FIG. 1. *An ensemble of 200 transient chaotic trajectories of Eq. (1) belonging to uniformly distributed initial points in the interval* $| x | < 0.5, y = 0$ *at the parameters* $a = 1.2715$, $b = 0.3$. *The chaotic attractor at these parameter values consists of seven pieces which fall in the x-projection on six separate intervals.*

Because of escape from any neighborhood of the chaotic saddle, the input of the procedure has to be an *ensemble* of time series of the preselected variable with several initial conditions and with endpoints on the true attractor[2], see Fig.1.

The use of an ensemble is of importance also because a few trajectories spending an exceptionally long time on the chaotic saddle do not necessarily generate the natural measure on this set but the ensemble does[2]. By following an ensemble of trajectories on the x-projection (Fig. 1.), six intervals are filled up with points of the asymptotic motion. One clearly sees also how the gaps in between become with increasing time less and less populated by the transients. The length of the densely populated region in the gaps gives a fairly good estimate to the averaged transient chaotic lifetime.

2. Locate the attractor of the dynamics in the variable investigated and separate the transient parts.

First, the attractor has to be localized on the x-projection. It is either a set of isolated points (in case of a periodic attractor) or a set of intervals (in case of a multipiece chaotic attractor), like e.g. in Fig. 1. That part of the trajectory which has not yet been settled down on the attractor is the transient component. It consists typically three regions (see Fig. 2.):

(I) Transient from the initial point to a neighborhood of the nonattracting chaotic set,

(II) motion in this neighborhood, and

(III) escape to the attractor.

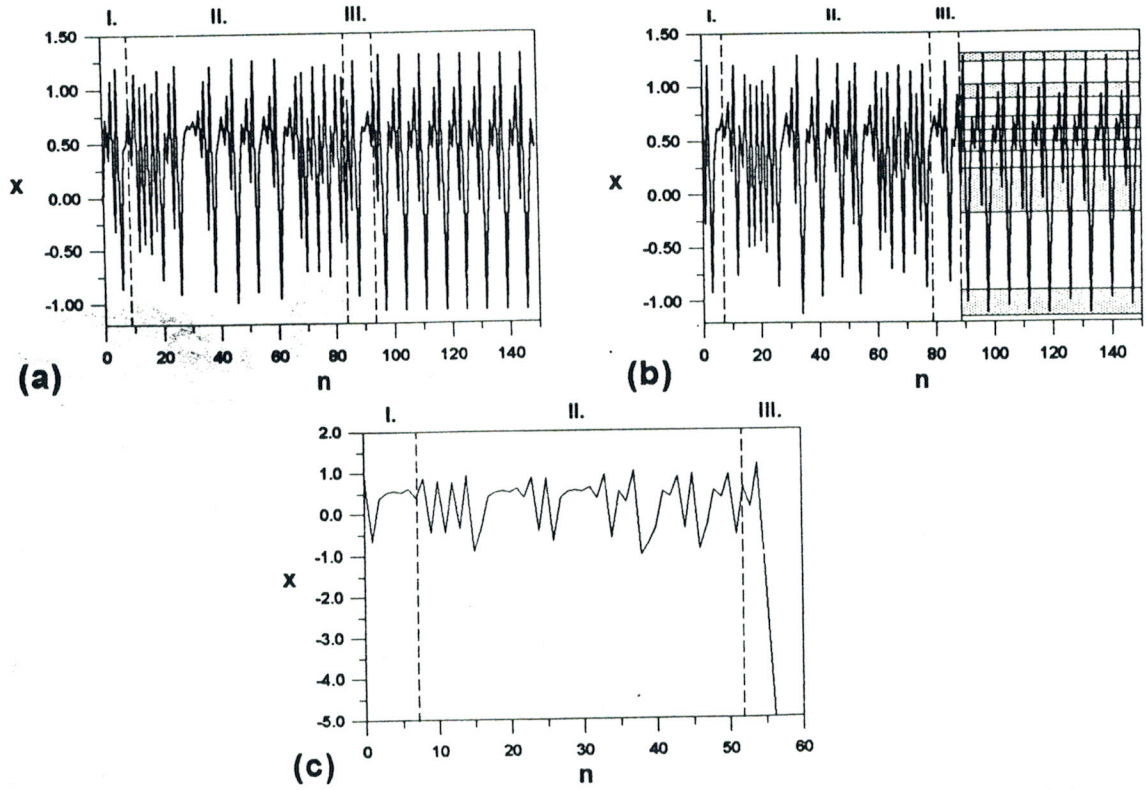

FIG. 2. *Typical transient signals generated by variable x of the Hénon map.* **(a)** *Signal settling down on a period-6 attractor,* $a = 1.240$, $b = 0.3$. *The intial point is* $x_0 = 0.92$, $y_0 = 0$. **(b)** *Signal settling down on a multi-piece chaotic attractor,* $a = 1.2715$, $b = 0.3$. *The initial point is* $x_0 = 0.06$, $y_0 = 0$. *The shaded stripes represent the projection of the 7-piece chaotic attractor to the x-axis.* **(c)** *Signal going to infinity at parameters* $a = 2.0$ *and* $b = 0.3$. *The starting point is* $x_0 = 0.930092, y_0 = 0$.

Regions I–III appear in any kind of transiently chaotic signals which, according to their asymptotic behavior, fall in one of the following categories (cf. Fig. 2).

(i.) Signals settling down on a periodic attractor. There is then rather easy to see when the attractor has been reached defining thus the endpoint of Region III. As an example, Fig. 2.a. shows a single typical transient chaotic signal of the x-component of the Hénon map at parameters $a = 1.24$ and $b = 0.3$. The attractor is a 6-cycle in this case.

(ii.) Signals settling down on a multi-piece attractor. A complication occuring in such cases is that in the single variable selected the attractor appears to be a union of intervals which might overlap with the projection of the chaotic saddle on this variable. When an element of the time series enters one of these intervals so that it never escapes later any projection interval of the attractor, the trajectory can still be close to the chaotic saddle. By taking the projection, however, some piece of information is lost, and we cannot do better than considering this element to be the endpoint of Region III in such cases. In Fig. 2.b. a transient signals of the Hénon map is plotted at parameter values $a = 1.2715$ and $b = 0.3$. In this case, the chaotic attractor consists of seven pieces, which fall in this projection on six separeted intervals.

(iii.) Signals settling down on an attractor lying far away from the chaotic saddle so that it can be considered to be at infinity. The endpoint of Region III is then defined by an x-coordinate which first falls out of a preselected interval covering the projection of the chaotic saddle. A typical transient signal is shown in Fig. 2.c. generated by the Hénon map again but at the parameters $a = 2.0$ and $b = 0.3$. The escape from the strange set is obvious by observing the very fast divergence to minus infinity where the attractor is situated.

3. Construct truncated time series, i.e., keep the points in Region II of the signal.

For the reconstruction of the nonattracting set, one only needs the points in Region II. This part of the signal will be called hereafter the *truncated time series*. There is, unfortunately, no well-founded way to choose the truncation limits. Therefore, it is to be checked whether the results depend on the cutoffs and one has to use a set for which this is not the case.

4. Glue the truncated signals together, apply a low-dimensional time-delay coordinate embedding, produce a Poincaré section, and plot the invariant set.

After cutting out those typically long parts of the signals which lie close to the attractor, as well as Regions I and III, an ensemble of truncated time series arises. The lengths of these truncated signals is in the order of the average transient life time. The next step is gluing together these pieces forming an *artificial time series* which represents "long time motion" in the neighborhood of the chaotic saddle. This time series can be analysed then by standard embedding techniques[9,10]. In sufficiently low dimensional cases, the geometrical form of the chaotic saddle can also be reconstructed.

In Fig. 3. we have plotted the first return map of a long artificial time series produced from 4000 truncated signals of the Hénon map at the parameter values of Fig. 2.c. A low dimensional object, the chaotic saddle is clearly observable together with some scattered points. These points (the cloud) are the consequence of the gluing procedure applied to produce the long time series. In order to understand the origin of the cloud we argue as follows. Take two truncated time series of the long signal (see Fig. 4.a). It is obvious that the jump between the endpoint of the first segment and the first point of the second segment

generate a cloud point which does not belong to a close neighborhood of the saddle. The next step is to avoid the appearance of the false Poincaré points so that we end up with a *single* long artificial time series each point of which is in close neighborhood of the chaotic saddle. (Note that such a signal can be considered as the time series analogue of a PIM-triple trajectory[3] which is an extremely long signal on a nonattracting chaotic set but available only in numerical simulations.) The use of it is more advantageous than that of many short truncated signals in a variety of potential investigations.

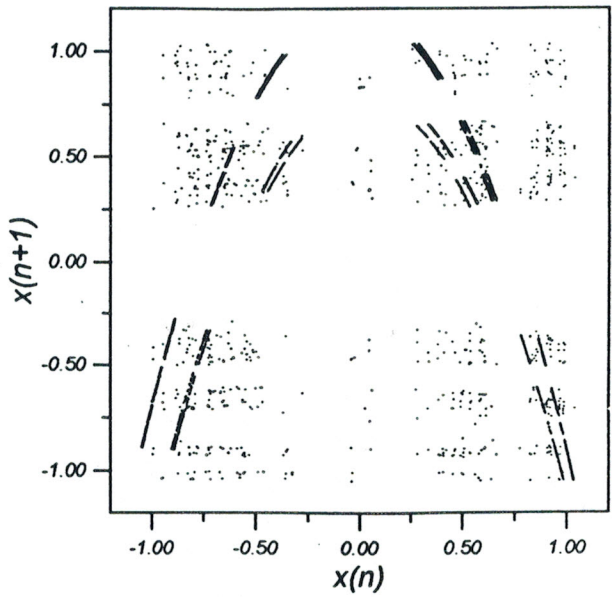

FIG. 3. *First return map of a long artificial time series generated by* 4000 *truncated signals of the Hénon map at parameter values* $a = 2.0$, $b = 0.3$. *The number of points discarded at the beginning (Region I) and before reaching the attractor (Region III) was chosen to be* 5 *and* 6, *respectively. The high density regions are parts of the chaotic saddle.*

5. Apply some simple matching procedure get rid of artificial points (the cloud).

A possible method to eliminate the cloud is demonstarted in Fig. 4.b, which is based on a matching of the truncated signals. An effective matching condition is the following: Choose a point in the truncated time series which has a value close enough to the endpoint of the previous segment, discard the intermediate points and glue the remaining part to the endpoint of the preceding segment.

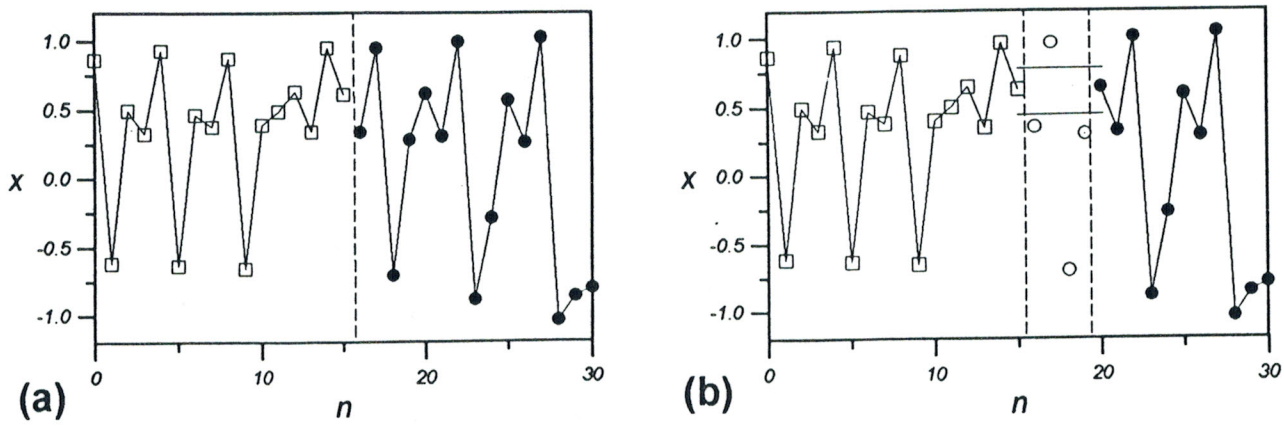

FIG. 4. (a) *Two short truncated time series of the time series used in constructing Fig.3. The gluing procedure is represented by a vertical line.* (b) *Illustration of the matching procedure. The points represented by open circles are discarded (see text).*

The result obtained in this way for the chaotic saddle is shown in Fig. 5. where the first return map of the time series of Fig. 3. is plotted after applying the matching condition: $x_g^{(n)} = x_e^{(n-1)} \pm b x_e^{(n-1)}$. Here $x_g^{(n)}$ is the gluing point of the n-th truncated time series, $x_e^{(n-1)}$ denotes the endpoint of the preceding segment and b is the allowed error range ($b = 0.1$ was taken when constructing Fig. 5). Almost all of the false cloud points disappeared.

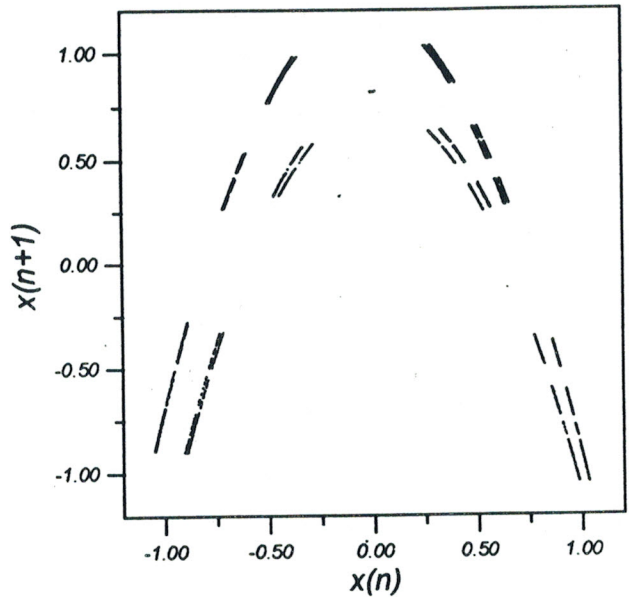

FIG. 5. *First return map of the time series of Fig. 3. after applying the single point matching condition with the value* $b = 0.1$ *(see text).*

Naturally, the matching process results in decreasing the number of data. A quantitative measure of this is the data reduction factor r which is the portion of data points that survived the matching procedure. Fig. 6. shows the dependence of the data reduction factor (r) on the matching errror (b).

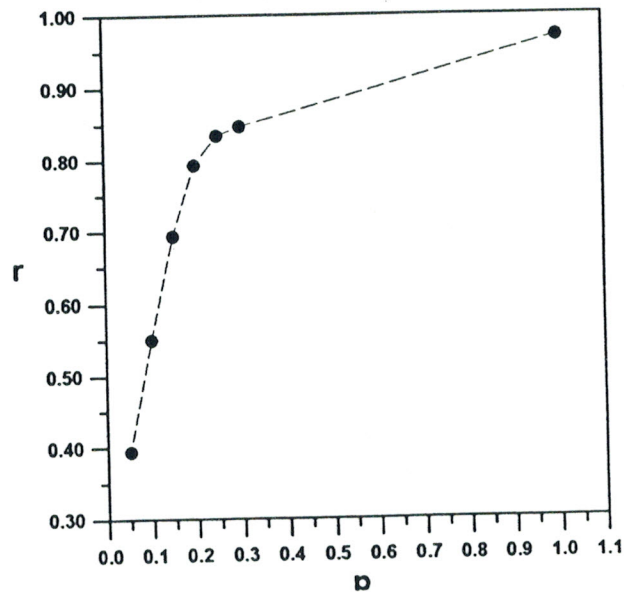

FIG. 6. *Data reduction factor (r) vs. different matching error values (b) applied to the ensemble of truncated time series used in Figs. 3. and 5.*

The form of the reconstructed invariant set can be compared with the chaotic saddle of the Hénon map obtained by a direct numerical simulation of the two-dimensional dynamics[3].

The agreement is fairly good with the exception of very tiny gaps which are not resolved in the reconstructed case. This is due to the uncertainty (which can be interpreted as a kind of noise) caused by the truncation and the matching procedures.

The algorithm can, of course, also be applied to cases where the attractor is close to the chaotic saddle. Figure 7. illustrates the result obtained at the parameters of Fig. 2.b. The applied matching error in Eq.(2) was $b = 0.15$. The thick and thin parts of the object represent the chaotic attractor and the chaotic saddle, respectively.

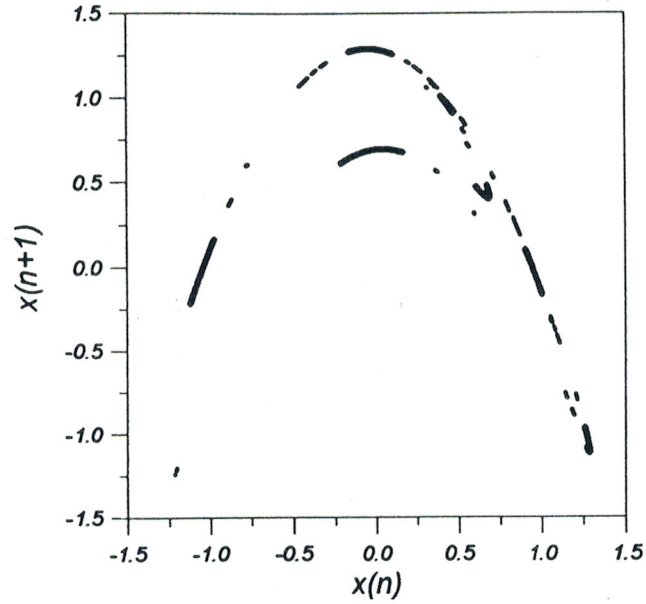

FIG. 7. *Reconstruction of the chaotic saddle (thin lines) of the Hénon map in the presence of a chaotic attractor (thick pieces). The parameters are* $a = 1.2715$ *and* $b = 0.3$. 4000 *truncated signals were used and the length of Region I and III was chosen to be* 4 *and* 5, *respectively. Cloud points have been filtered out by using the matching procedure with* $b = 0.15$.

6. Apply the usual time series analysis method to determine quantitative characteristics of the chaotic saddle like, e.g. dimensions.

As a next step of the time series analysis, one can determine, for example, the dimension of the chaotic saddle. There are several well known methods for measuring the dimension of a fractal object, such as the simple box counting method[8] or the correlation dimension calculation[9]. In order to compare the two methods we carried out several calculations. An example is shown in Fig. 8. for the case when the attractor is a 6-cycle. The number of two-dimensional boxes $N(\epsilon)$ of linear size ϵ needed to cover the chaotic saddle is plotted in Fig. 8.a. The best power fit yields the dimension $D_{box} = 1.05 \pm 0.1$. The relatively large error comes from the unavoidable effect that one does not reconstruct the saddle directly from a dynamics but rather from an artificial time series which is subject to errors partially becuase of testing a close neighborhood of the nonattracting chaotic set only. Fig. 8.b. shows the result obtained via the embedding technique. A phase point $\vec{p_i}$ is defined by the d-dimensional time delay vector

$$\vec{p_i} = \{x_i, x_{i+1}, \ldots, x_{i+d-1}\} \quad ,$$

as usual[9]. The correlation sum $N(r)$ is obtained by counting the number of neighboring phase points which are closer to each other than a distance r:

$$N(r) = \{\text{number of pairs} : |\vec{p_i} - \vec{p_j}| < r\}.$$

In the scaling region $r \ll 1$, the correlation dimension D_{cor} is given by the exponent of the best power fit to the correlation sum $N(r)$ vs. r. As is clearly seen in Fig. 8.b., the embedding process is characterized by correlation sums the graphs of which run parallel to each other on a log-log plot for $2 \leq d \leq 5$. The correlation dimension extracted from them is $D_{cor} = 1.07 \pm 0.05$. The procedure proved to be reliable by comparing the results obtained in this way with those of a direct dimensional calculation of the Hénon saddle.

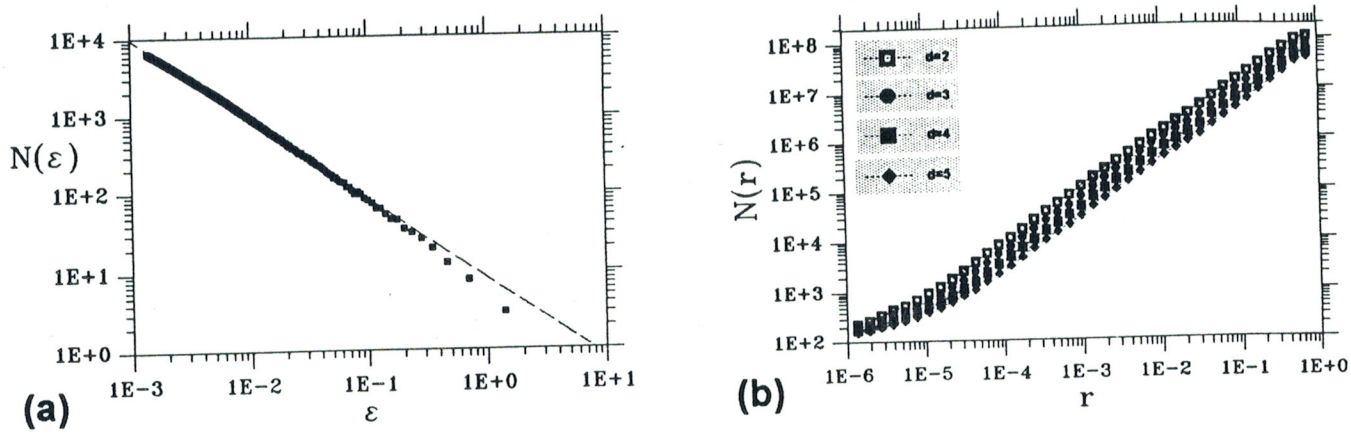

FIG. 8. **(a)** *Result of the box-counting calculation of the chaotic saddle at parameters* $a = 1.240$ *and* $b = 0.3$ *(the case of Fig. 2.a). The slope of the dashed line is* -1.05. **(b)** *Correlation sum for the same strange set. The slope of the parallel straight line segments is* 1.07.

III. CONCLUDING REMARKS

The experimental investigation of transient chaos has received disproportionately little attention (for a few examples see [11]–[22]) and, with the exception of a very recent effort[23], has mainly concentrated on determining the averaged chaotic lifetime. In this paper we illustrated that, apart from natural modifications, transient chaos can be analysed from time series in very much the same manner as permanent chaos. By means of the procedure described above chaotic saddles underlying transient chaotic dynamics can be reconstructed and their characteristics taken with respect to the natural measure can be determined from time series. To our knowledge, this has not yet been carried out in any laboratory experiments where the equations of motion of the system are not known.

IV. ACKNOWLEDGEMENTS

This work has been supported by the Soros International Foundation and the Hungarian National Science Foundation (OTKA) under Grant No. 2090, No. 2091, No. T4439, and by the Foundation for Hungarian Higher Education and Research.

---

[1]C. Grebogi, E. Ott and J. Yorke, Phys. Rev. Lett. 48, 1507 (1982); Physica (Amsterdam) D 7, 181 (1983).

[2]H. Kantz and P. Grassberger, Physica (Amsterdam) **D 17**, 75 (1985).

[3]H. E. Nusse and J. Yorke, Physica (Amsterdam) **D 36**, 137 (1989).

[4]T. Tél, in *Directions in Chaos, Vol. 3*, ed. Hao Bai Lin (World Scientific, Singapore, 1990) p. 149.

[5]C. Grebogi, E. Ott and J. Yorke, Phys. Rev. **A 36**, 3522 (1987).

[6]P. Cvitanovic, Phys. Rev. Lett. **61**, 2729 (1988).

[7]T. Tél, J. Phys. **A 22**, L691 (1989).

[8]T. Vicsek, *Fractal Growth Phenomena* (World Scientific, Singapore, 1989).

[9]P. Grassberger, I. Proccacia, Physica (Amsterdam) **D 9**, 189 (1983).

[10]*Proceedings of the 1st Experimental Chaos Conference*, eds.: S. Vohra et al., World Scientific, Singapore, 1992; *Proceedings of the IUTAM Symposium and NATO Advanced Research Workshop on the Interpretation of Time Series from Nonlinear Mechanical Systems, University of Warwick, England, 26-30 August 1991*, eds.: P. G. Drazin and G. P. King, Physica (Amsterdam) **D 58**, Nos. 1-4 (1992).

[11]V. Croquette and C. Poitou, C. R. Acad. Sc. Paris **292**, 1353 (1981).

[12]F. T. Arecchi, R. Meucci, G. Puccioni and J. Tredicce, Phys. Rev. Lett. **49**, 1217 (1982).

[13]P. Bergé and M. Dubois, Phys. Lett. **A 93**, 365 (1983).

[14]F. T. Arecchi and F. Lisi, Phys. Rev. Lett. **50**, 1330 (1983).

[15]R. W. Rollins and E. R. Hunt, Phys. Rev. **A 29**, 3327 (1984);
R. C. Hilborn, Phys. Rev. **A 31**, 378 (1985).

[16]R. W. Leven, B. Pompe, C. Wilke and B. P. Koch, Physica (Amsterdam) **D 16**, 371 (1985).

[17]M. Gorman, P. J. Widmann and K. A. Robbins, Phys. Rev. Lett. **52**, 2241 (1984); Physica (Amsterdam) **D 19**, 255 (1986);
P. J. Widmann, M. Gorman and K. A. Robbins, Physica (Amsterdam) **D 36**, 157 (1989).

[18]T. L. Carroll, L. M. Pecora and F. J. Rachford, Phys. Rev. Lett. **59**, 2891 (1987); Phys. Rev. **A 40**, 377; 4149 (1989); J. Appl. Phys. **64**, 5396, (1988);
T. L. Carroll, F. J. Rachford and L. M. Pecora, Phys. Rev. **B 38**, 2938 (1988).

[19]Z. J. Kowalik, M. Franaszek and P. Pieranski, Phys. Rev. **A 37**, 4016 (1988).

[20]F. Papoff, D. Dangoisse, E. Poite-Hanoteau and P.Glorieux, Optics Comm. **67**, 358 (1988);
D. Dangoisse, P. Glorieux and D. Hennequin, Phys. Rev. Lett. **57**, 2657 (1986).

[21]W. L. Ditto et al., Phys. Rev. Lett. **63**, 923 (1989).

[22]R. Stoop and J. Parisi, Phys. Rev. **A 43**, 1802 (1991).

[23]R. W. Leven, M. Selent, and D. Uhrlandt, private communication.